Open Access

Cosmogenic [10]Be and OSL Dating of Marine Terraces Along the Central-East Coast of Korea: Spatio-Temporal Variations in Uplift Rates

Soo Yong Lee[1,3], Yeong Bae Seong[*,1], Hee Cheol Kang[2], Kwang Hee Choi[3] and Byung Yong Yu[4]

[1]*Department of Geography Education, Korea University, Seoul, Korea*

[2]*Institute of Environmental Geosciences, Pukyong National University, Pusan, Korea*

[3]*Environmental Resources Research Department, National Institute of Environmental Research, Incheon, Korea*

[4]*Korea Institute of Science and Technology, Seoul, Korea*

Abstract: We report the abandonment age of the Jeongdongjin (JDJ) coastal terrace that lies at 65 m a.s.l. The age of the JDJ terrace surface has yet to be equivocally constrained because of its antiquity (>MIS 5), challenging the application of conventional radiocarbon and optically stimulated luminescence (OSL) dating techniques. The reliability of applied indirect age constraints on the sediments by amino-acid racemization and tephra chronology is debated. We present the first application of cosmogenic surface exposure dating to constrain the age of the old terrace in Korea. We dated four samples from the paleo shore platform surface using cosmogenic [10]Be surface exposure dating techniques. The analyses yielded exposure ages ranging from 240 to 170 kyr and likely correspond to the penultimate interglacial period (MIS 7). Sandy beach sediments overlying marine terraces at nearby Anin (~23 m a.s.l.) and Ayajin (~17 m a.s.l.) were dated by OSL. OSL dating of terrace beach sand in two separate areas yielded ages between 129–117 and 70–66 kyr, interpreted MIS 5e and MIS 5a, respectively. Combining the exposure ages and the heights of terraces corrected for paleo sea level, we obtain uplift rates of 353 for JDJ, 159 for Anin, and 238 mm/kyr for Ayajin. The results indicate spatio-temporal variations in the rate of surface uplift along the east coast of Korea during the late Quaternary. Furthermore, the west and east coasts of central Korea experienced different uplift histories during the late Quaternary, possibly resulting from the effects of different tectonic regimes.

1. INTRODUCTION

Since the first report on the coastal terrace of the Jeongdongjin (JDJ) by [1], the JDJ surface has been a key area for coastal terrace stratigraphy as well as an important teaching example in Korea. However, although many direct and indirect dating methods have been applied to constrain the age of the JDJ, the age of the terrace surface remains debated. Methods of direct dating include optically stimulated luminescence (OSL) and indirect dating include amino-acid racemization [2, 3], tephra chronology [4, 5], and morphostratigraphy using a weathering index and soil development [3, 4].

Dating by OSL has not yet been successful in constraining the age of the JDJ because the sediments are old, resulting in a high dose rate and consequent oversaturation of the OSL signal. To overcome this impedance, a new luminescence technique that analyses feldspar, known as infrared stimulated luminescence (IRSL), has been employed [2]; however, the reliability of the method requires further research to determine the suitability

of the feldspar signal [6, 7]. Surface exposure dating using cosmogenic [10]Be has been successfully applied to coastal terraces and other geologic surfaces [8, 9]. In this study, we firstly completed conventional cosmogenic surface exposure dating to constrain the age of the old (>MIS 5) terrace surface in Jeongdoinjin (JDJ) and secondly applied OSL dating to nearby lower terraces in Anin and Ayajin (<MIS 5). Using these data, we estimate the uplift rate for each coastal terrace and reconstruct the spatio-temporal pattern of uplift in central and eastern Korea.

2. STUDY AREAS

2.1. Physiographical Setting

The Korean Peninsula is located along the eastern margin of Eurasia and is adjacent to the western Pacific Ocean. The peninsula belongs to the temperate zone, having four distinct seasons. During the winter, from December to February, the peninsula is affected by the Siberian High pressure system, rendering the area cold and dry. Conversely, the summer, from June to August, is hot and humid with frequent heavy rainfall derived from the East Asian monsoon. The present study areas are situated in central-east Korea, ~250 km east of Seoul (Fig. **1**). Topographically, the study areas lie within the boundary between the coastal plain area and the hill area

*Address correspondence to this author at the Department of Geography Education, Korea University, Anam-Ro 5Ga, Seongbuk-Gu, Seoul, Korea; Tel: +82232902367; Fax: +82232902360; E-mails: ybseong@korea.ac.kr, ybseong@hotmail.com
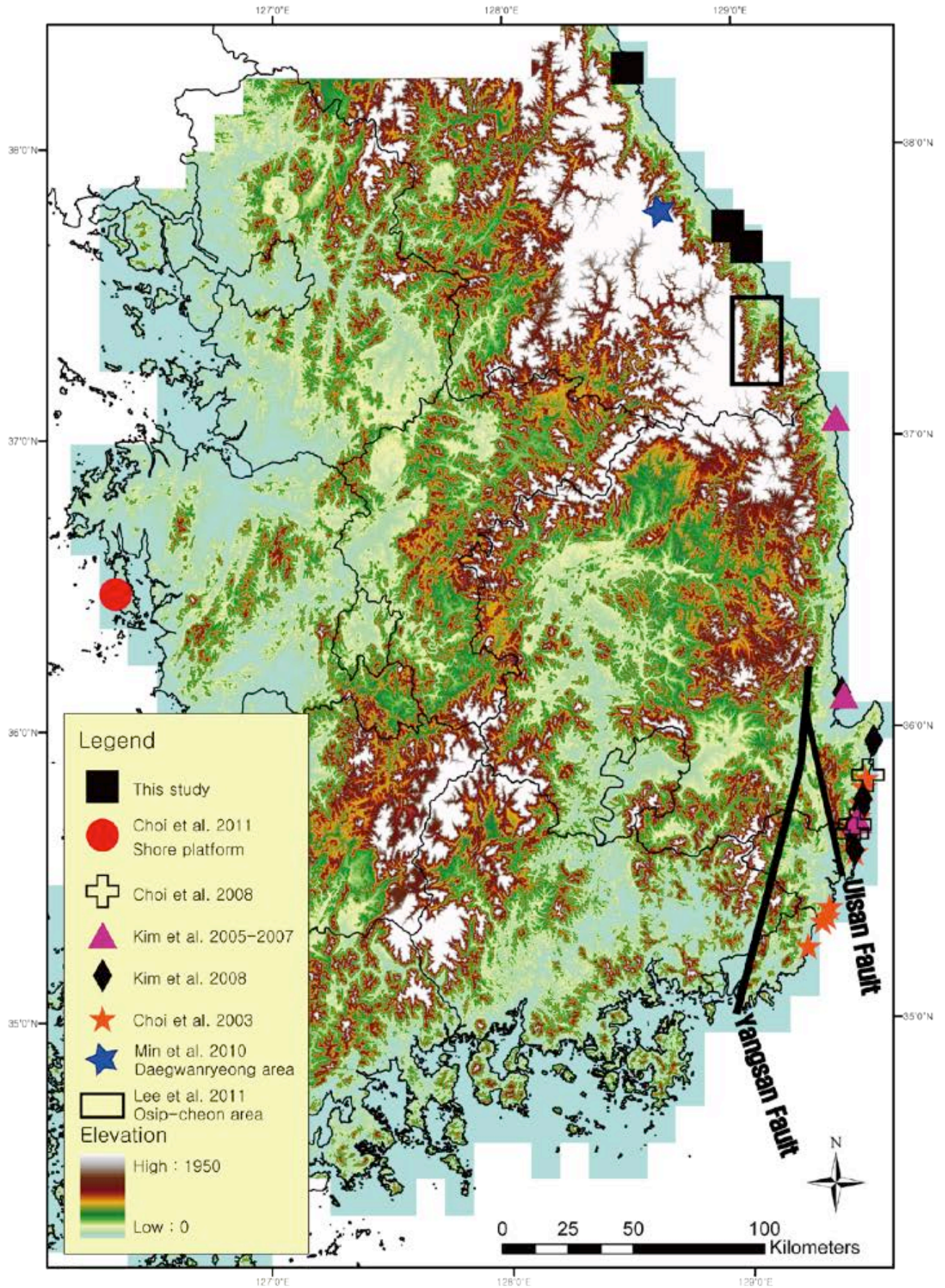
Fig. (1). Regional digital elevation model (constructed from a 1:25,000 topographic map) showing the location of the three study areas and other key areas where uplift rates have been calculated previously.

in the western mountainous area of the Taebaek Mountains, located within the backbone of the Korean Peninsula. This area has extensive flights of coastal terraces along the east coast. The marine climate of the study area is characterized by a cool, humid summer and warm winter. In the Gangneung area, the mean annual temperature is 13.1°C, and the mean temperatures in August and January are 24.6°C and 0.4°C, respectively. Precipitation is relatively high, averaging 1687.7 mm/yr, with about 60% of the annual precipitation occurring between the months of June and August [10]. In winter, there is a substantial amount of precipitation compared with the west of the Taebaek Mountains due to the advection of humid air flow crossing the East Sea/Sea of Japan from eastern Siberia.

Lithologically, the study area consists of the Carboniferous to Early Triassic Pyeongan Supergroup, Jurassic biotite-granites, late Miocene basalts, and Quaternary coastal terrace deposits and alluvium (Fig. **2**). The Pyeongan Supergroup unconformably overlies the Cambro-Ordovician Joseon Supergroup and consists mainly of siliciclastic sediments with several coal seams. The Pyeongan Supergroup is divided into three parts: Lower (Carboniferous Hongjeom Series), Middle (Permian Sadong Series), and Upper (Early Triassic Gobangsan Series) (Fig. **2A**).

In the Ayajin a Jurassic biotite-granite body known as the Bulguksa granite occupies most of the mapped area (Fig. **2B**). This single batholith intrusion is medium- to coarse-grained. The late Miocene basaltic rocks outcrop as a lava-dome at the summit of several small mountains. The basalt is characterized by columnar jointing and contains a porphyritic texture with megacrysts of pyroxene (Fig. **2B**).

In the area of Gangneung, the present-day direction of maximum horizontal compression is approximately N70–80°E, and the compression is accommodated by either strike-slip or reverse movement along the Imgok fault (Fig. **2A**; [11-13]). Faults located in the terrestrial (western) part of the study area commonly occur as thrust and strike-slip faults. The faults were active until the late Miocene and several were likely reactivated during the Quaternary [14, 15]. East to the study area, the Gangneung Fault trending parallel to the coast, occurs as a normal fault that was initiated during the opening of the East Sea/Sea of Japan, but in its present state is likely accommodating movement resulting from inversion tectonics associated with shortening of the East Sea ([16]; Fig. **3**).

2.2. Terraces and Sampling Locations

Multiple flights of terraces with elevation from ~ 5 m a.s.l. to ~70 m a.s.l. are present along the east coast of Korea [3, 17-21]. Within the study area, coastal terraces occur at three different levels (60-70, 20-30, and 10-20 m a.s.l.), which are mostly consisting of gravel and sand deposits. Most of clasts are substantially weathered (breakable by hand) (Fig. **4**). A well-sorted marine deposit (~3 m thick) representing the low terrace surface (~20 m a.s.l.) is exposed throughout the Ayajin area (Fig. **5**). The stratigraphic section consists of a weathered, unknown bedrock base, a pebble to cobble deposit with a coarse sand layer, a sand deposit with a granule layer, silt, and a recent soil.

The JDJ coastal terrace is categorized into two treads with different heights [1]. The present study is focused on the lower tread which have been focused by previous works
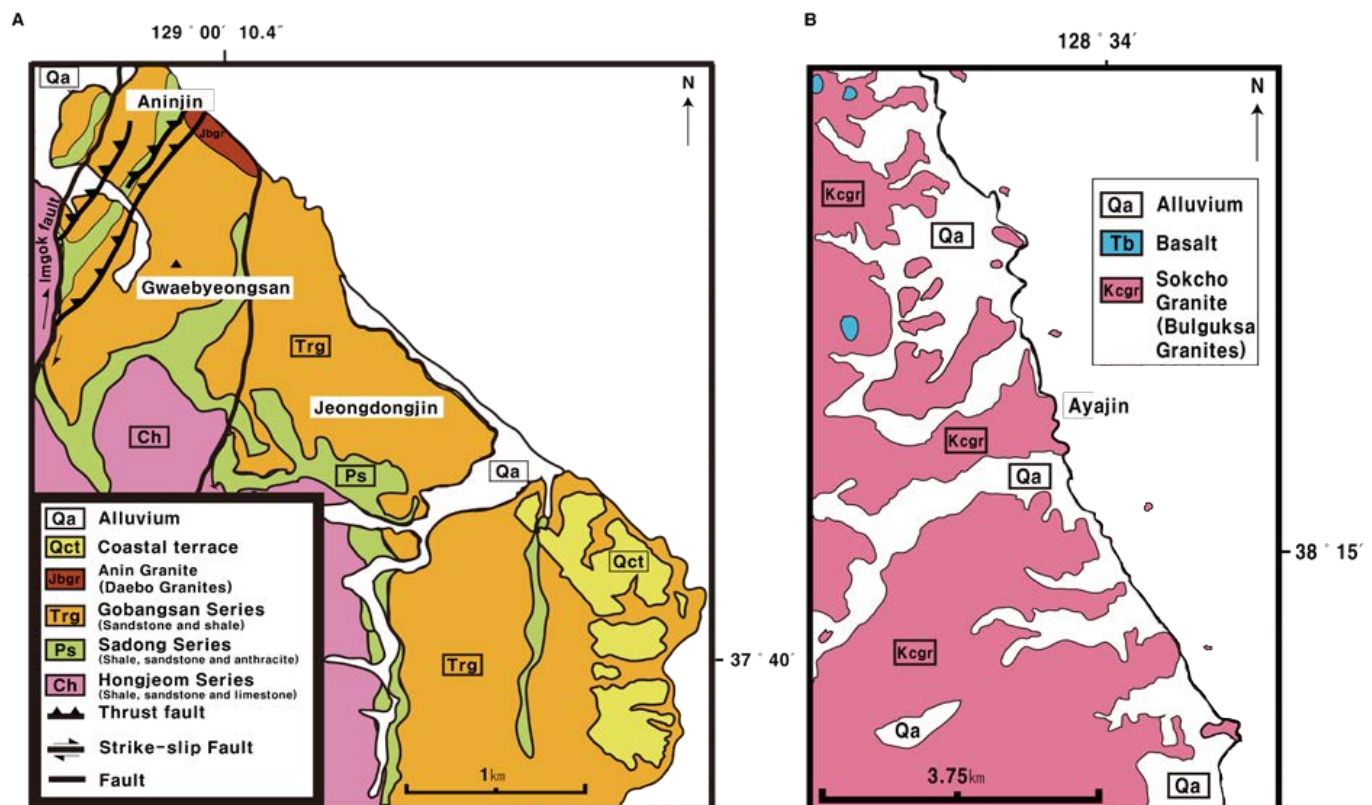

Fig. (2). Geological maps of study areas [53]. (**A**) is for Jeongdongjin and Anin and (**B**) for Ayajin.
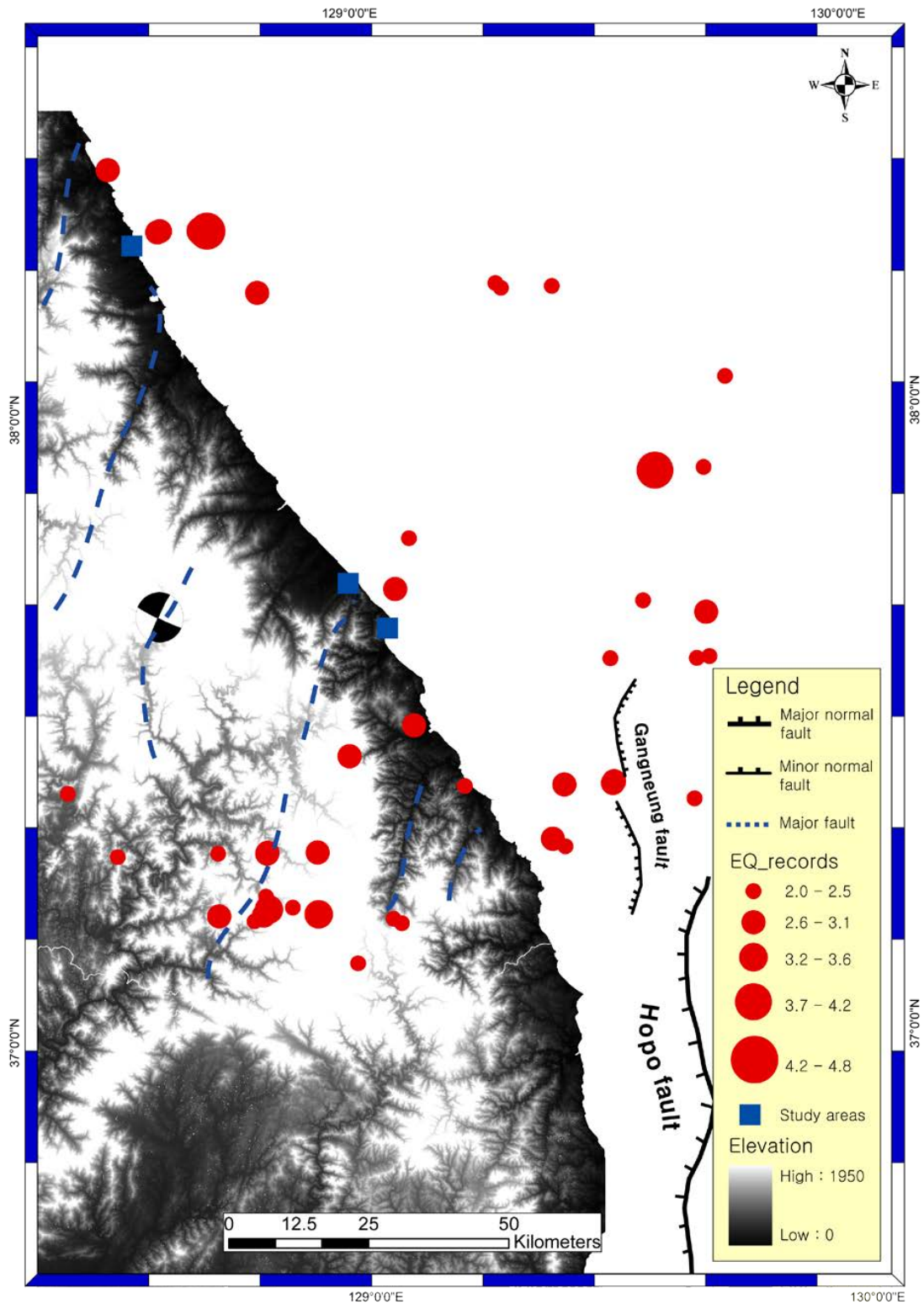
Fig. (3). Tectonic map showing the occurrence and magnitude of earthquakes since 1980 (from the Korea Meteorological Administration, 2010).

[2-5]. Extensive (~100 m in width) and gently dipping (<1°) terrace surfaces (exposed at 60–70 m a.s.l. along the coast) preserve multiple pits created by shell-boring, which live on the bedrock in and shallow (< ~5 m) sea level and are likely to be interpreted evidence of a paleo shore platform (Fig. **4**). Such pits are found along shore platforms at the present sea level, implying the terrace shore platform was located near to the paleo sea level (Fig. **6**). Locally, the terrace exposes well-rounded, disk shape of beach gravel deposits that are interbedded with well-sorted, texturally mature sand deposits (Figs. **5**, **7**).
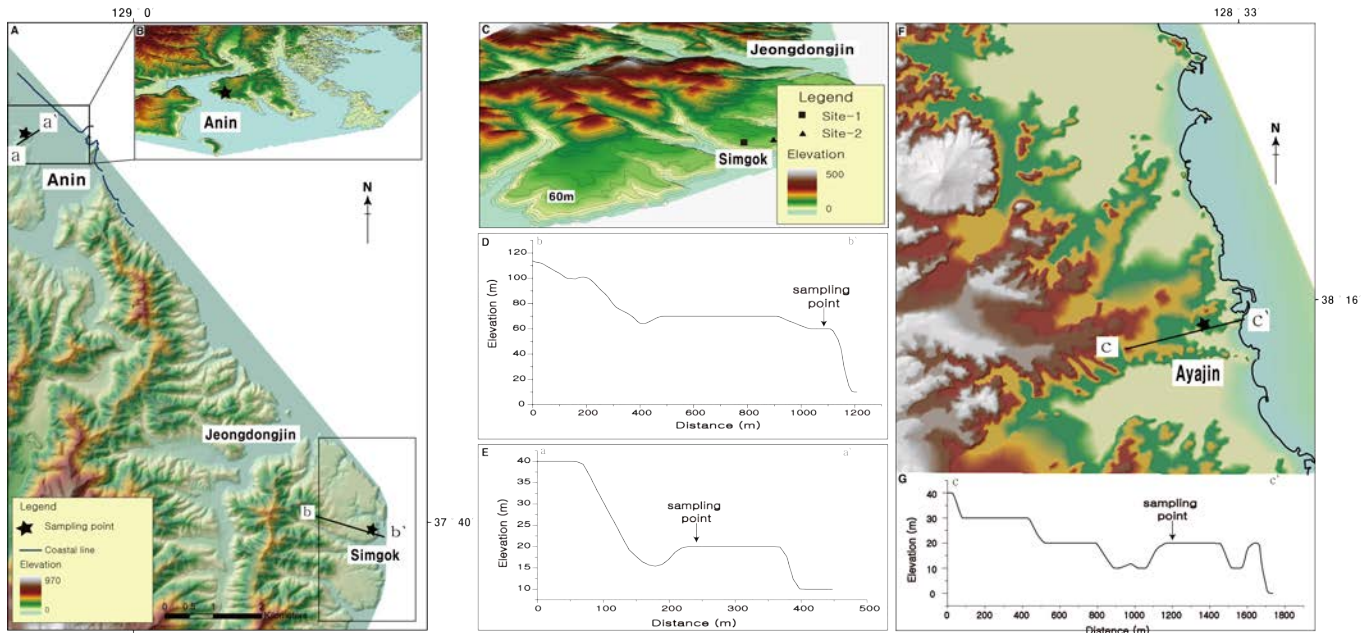
Fig. (4). Map of marine terraces in the Jeongdongjin (JDJ) and Anin regions. (**A**) The most prominent 20 m and 70 m terraces occur throughout most of the JDJ and Anin regions, which generally are broad and overlain by thick marine deposits. (**B**) Birds-eye views of the two areas (Google Earth image). The filled square in (**A**) indicates the paleo shore platform (Site-1; JDJ 103, 104) which contains fossilized hollows from shell-borings. The filled triangle indicates Site-2 (JDJ 201, 202). Elevations of sampling points were calculated by Trimble total station. The shell-boring hollows are found only at Site-1 (see Fig. **5A**, **B**). (**C**) Birds-eye view of the Jeongdongjin (JDJ) terrace and sampling locations. (**D**) Elevation profile of Anin terrace along a-a`. (**E**) Elevation profile of JDJ terrace along b-b`. (**F**) Digital Elevation Model of Ayajin area. (**G**) Profile showing elevation change of Ayajin terrace along c-c`.
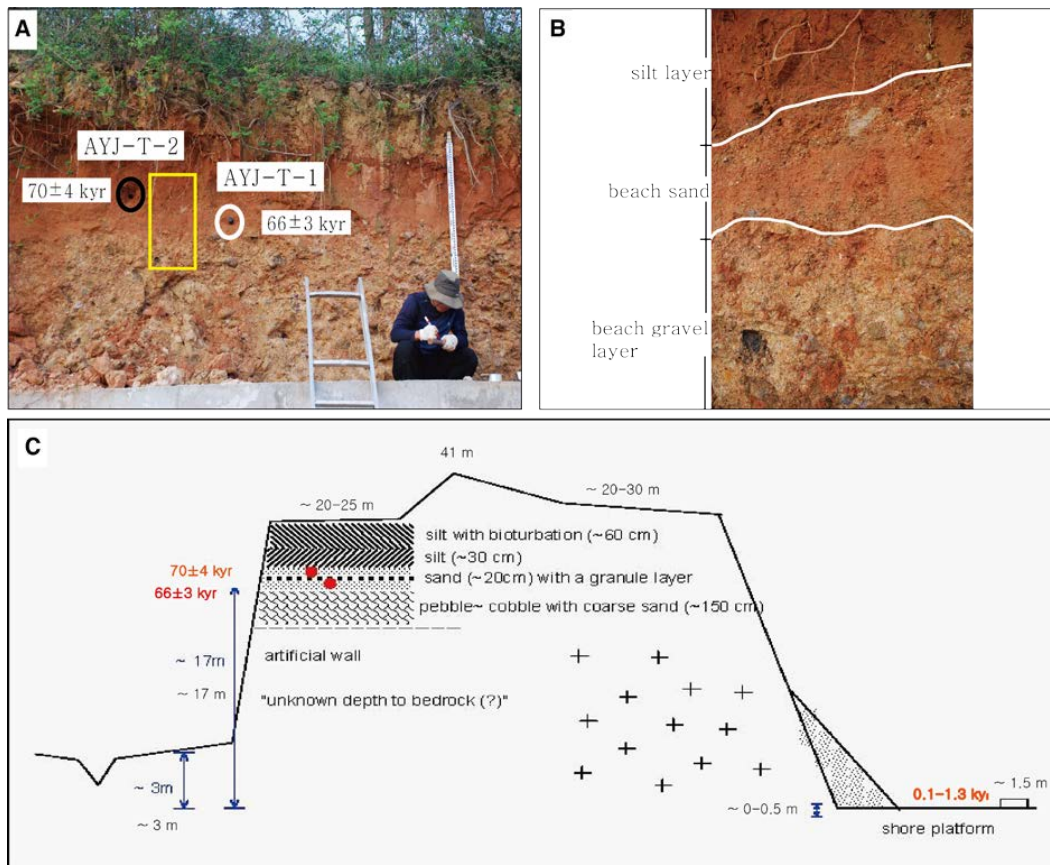

Fig. (5). Field photographs of sampling sites and a cross-section of the terrace in the Ayajin (AYJ) area. The white and black circles in (**A**) indicate the sampling locations for OSL dating, which yielded exposure ages of 66 and 70 kyr, respectively, and a yellow box are enlarged in (**B**). (**C**) Cross-section of the AYJ beveled coastal terrace (~20 m a.s.l.), showing a columnar section of the exposure sampled for OSL dating.
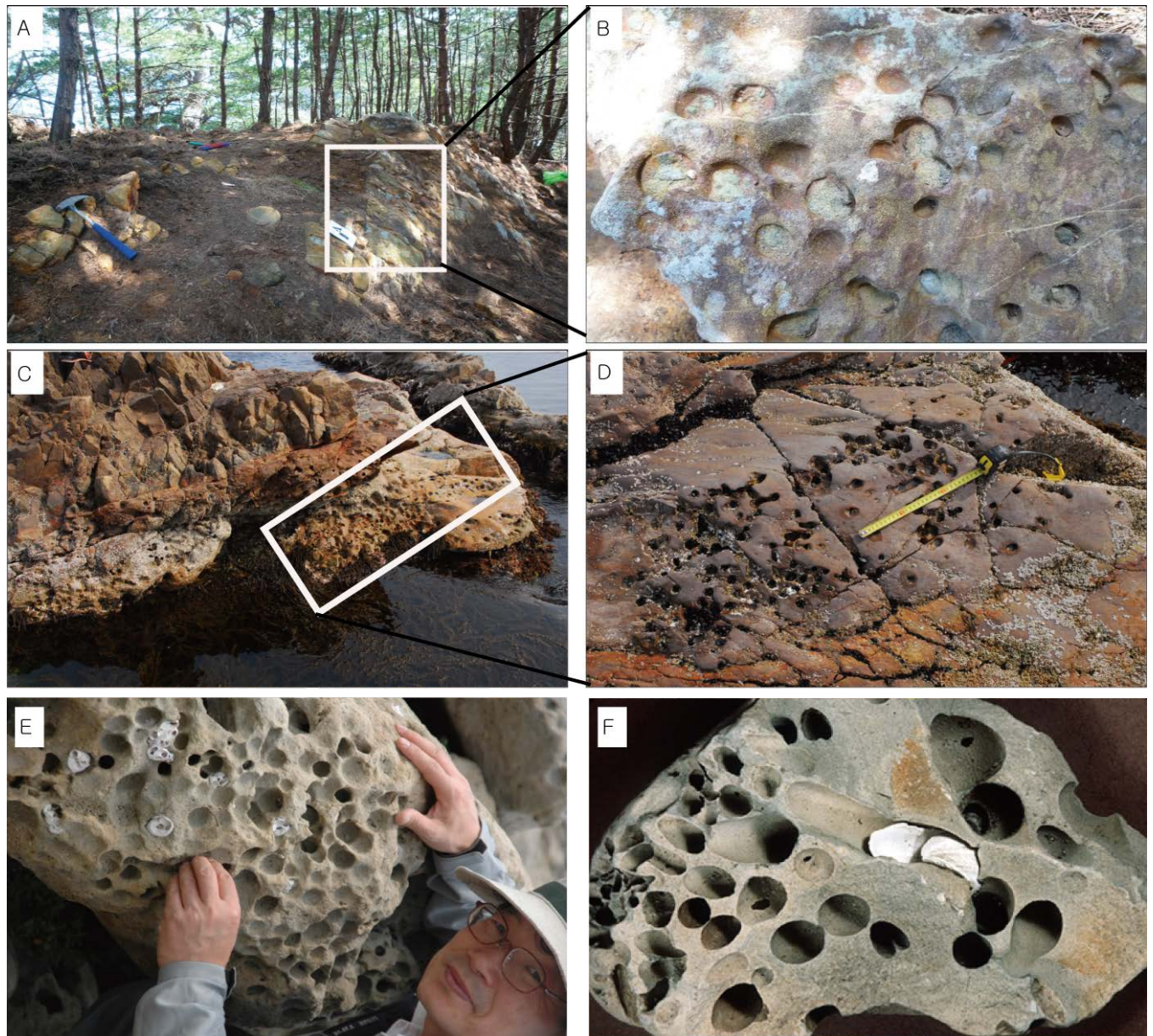
Fig. (6). Field photographs of paleo shore platforms (**A**, **B**) and present shore platforms of study area (**C**, **D**), all of which contain pits, indicating that they were engraved onto the shore platform near to the sea level. Pictures showing an example of rock-boring shell in Korean coast (**E**; *Zirfaea subconstricta*; [54]) and in Oregon coast (**F**; (*Penitella penita*)). The latter one is reported to erode the rock surface at an average rate of 0.5 mm/yr and up to 12 mm/yr [55].

Excellent exposures of marine deposits overlying the middle terrace surface (~23 m a.s.l.) are found in the Anin area (Fig. **7**). The ~4-m-thick sedimentary section consists of four units: bedrock, marine gravel, beach sand, and recent soil. The soil is yellow and reddish, indicating substantial weathering and soil formation since the abandonment of the terrace.

The marine terraces are characterized by gentle treads and steep cliffs that were formed by wave erosion. The terrace tread, beveled by wave erosion, is abandoned and exposed to cosmic rays. If the abundances of cosmogenic [10]Be from the marine terrace treads are determined, the apparent minimum exposure duration of the treads can be calculated. Four samples for cosmogenic [10]Be surface

exposure dating were collected from the outer exposed bedrock edge of JDJ terrace surface and the elevation at each of the target locations was measured using a total station. The degree of weathering and the site-specific conditions at each sample location were recorded. Topographic shielding was determined by measuring the inclination from each sample site to the top of surrounding mountain ridges and peaks. Samples were collected by hammering off a layer (1–5 cm thick) of quartz-rich bedrock on top of the intact surface at each sample location.

3. METHODS

All the samples were prepared at the Geochronology Laboratory at Korea University, Seoul, Korea. First, the
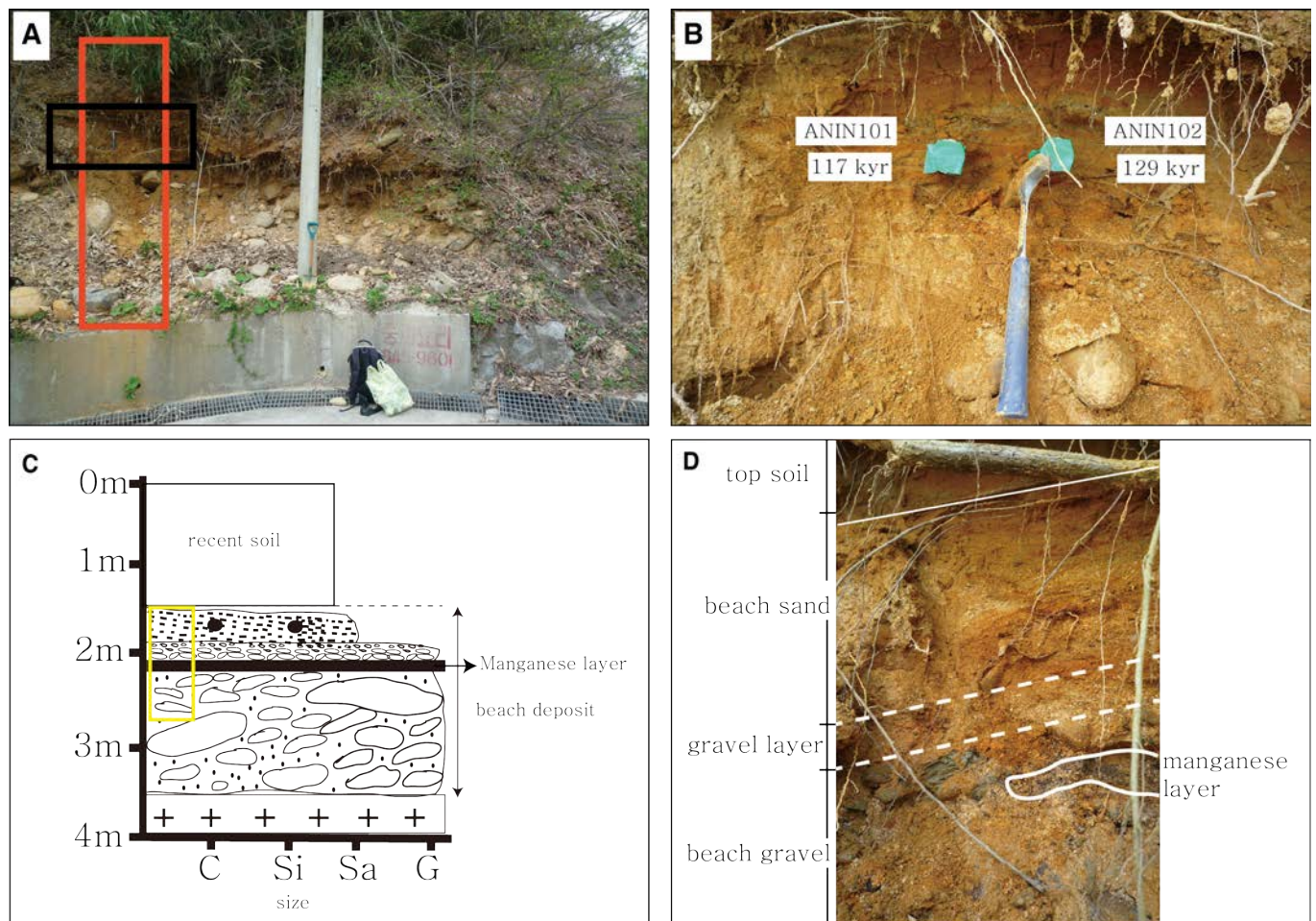
Fig. (7). Stratigraphy of the ~4-m-thick sediment associated with the ~25 m a.s.l. marine terrace in the Anin area. (**A**) The stratigraphic section consists of bedrock, marine deposit, beach sand, and recent soil. A black rectangle indicates the locations from which samples for OSL dating were taken and is enlarged as panel **B**. (**B**) Snapshot of the sampling location of OSL dating and each OSL age. The material consists of well-rounded, well-sorted beach sand. (**C**) Columnar section of an exposure of the Anin coastal terrace. Yellow box is enlarged in (**D**) to show the detailed sedimentary facies.

samples were crushed and sieved and then separated into 250–710 μm size fractions following the standard method proposed by [22]. After the addition of low-background ($^{10}Be/^9Be < 10^{-15}$) ^9Be carrier, Be was separated and purified by ion exchange chromatography and precipitated at pH > 7. Hydroxides were oxidized by ignition in quartz crucibles. BeO was mixed with Nb metal and loaded onto targets for measuring the $^{10}Be/^9Be$ ratio by accelerator mass spectrometry (AMS) at the Korea Institute of Geology and Mineralogy (KIGAM), Daejeon, Korea. Isotope ratios were normalized to the ^{10}Be standards prepared by [23] using a ^{10}Be half-life of 1.387×10^6 yr [24, 25]. The measured isotope ratios were converted to cosmogenic ^{10}Be concentrations in quartz using the total ^{10}Be in the samples and the sample weights. Cosmogenic ^{10}Be concentrations were then converted to minimum surface-exposure ages using the CRNOUS exposure age calculator (version 2.2; [26]), which utilizes scaling factors after [27, 28] and a density of 2.7 g/cm^3. The error ranges for the exposure ages in this study are shown as 2 standard deviations (e.g., ± 2σ) and account for external uncertainties including measurement and production rate uncertainties).

OSL dating was applied to determine the depositional ages of the Ayajin and Anin terraces. This method offers a feasible method of accurately determining the timing of sediment deposition. Two samples at each locality were collected from marine terrace sediments at 23.08 m a.s.l. (Anin area) and at 17.00 m a.s.l. (Ayajin area). The samples were obtained by driving a stainless pipe, 25 cm in length and 7 cm in diameter, into the freshly exposed sand walls of the profile. After the sample was retrieved, the end of the pipe was instantly capped with aluminum foil and the sample stored in a dark container. The samples were prepared and analyzed at the Korea Basic Science Institute (KBSI), Ochang, Korea using the single-aliquot regenerative-dose (SAR) protocol [29]. The recently developed SAR protocol for the optical measurements of quartz has resulted in an improved precision and accuracy for age determinations [29, 30]. In the laboratory, the samples were wet sieved to recover the 90–250 μm size fractions, and cleaned in 10% H_2O_2, 10% HCl, and 40% HF. These fractions were pretreated for the preparation method of the SAR protocol [31]. All OSL measurements were performed using an automated Risø TL/OSL measurement system. Error is yielded based on saturated water contents.

4. RESULTS

JDJ terrace was dated by cosmogenic [10]Be and Ayajin and Anin terraces were dated by OSL dating for the present study. The JDJ coastal terrace can be divided into two sites (Site-1 and Site-2 at Fig. **4**). Two samples (JDJ103 and JDJ104) were collected from Site-1, situated at the outer edge of JDJ terrace. Sample JDJ103, at 65 m a.s.l., yielded an age of 211.17 ± 20.73 kyr, and JDJ104 at 65 m a.s.l. yielded an age of 159.94 ± 23.36 kyr. Two samples collected at Site-2 yielded exposure ages of 224.69 ± 30.83 kyr (JDJ 201) and 253.69 ± 27.72 kyr (JDJ 202). The exposure ages of terraces at JDJ range from 254 to 160 kyr (Table **1**) and without an outlier (JDJ-204) broadly correspond to the penultimate interglacial period (MIS 7). When considering the effect of surface erosion on the abundance of cosmogenic [10]Be, the surface may be older (i.e., MIS-9). The intact geometry of pits on the surface may imply that there has been little erosion and/or weathering on the exposed surface since the abandonment of terrace. In the meantime, covering materials such as aeolian dust might be deposited on the surface, possibly reducing the real exposure duration of the surface which yield underestimation of real age. However, the sampling location is on the outer edge of the long and wide terrace tread, where any dust deposit is difficult to reside longer in situ. Hence we prefer the intact marks of shell-boring on the dated surfaces to suggest that the results represent the age of surface formation although we cannot exclude any possibility of underestimation of the real abandonment age of the terrace related to surface erosion and aeolian covering.

The OSL ages derived from the Ayajin and Anin marine sediments represent the timing of deposition. In the Ayajin area, OSL dating of two samples (AYJ-T-1 and AYJ-T-2) from pocketed terrace beach sand taken from horizontally similar elevations (17 m a.s.l.) yields dates of 66 ± 3 kyr and 70 ± 4 kyr, respectively (Fig. **6**). This time frame of ~67 kyr corresponds to a glacial period (MIS 4) when the sea level was as low as 18 to 30 m b.s.l. [32]. The beach sediment is usually younger than the underlying, wave-cut platform and the eustatic sea level change is spatially variable [33] and the recurrence interval of large earthquakes in intraplate regions

is relatively long (1000–10,000 years; [34]). Furthermore the present OSL ages may be underestimated with saturation. The equivalent dose rate of our samples is more than 300 Gy (Table **2**) whereas OSL signal of quartz is generally considered to have reached at the saturated range. Lastly, during the last glacial period, the study area was under the periglacial condition, possibly causing the underestimation of OSL age by mixing with down-ward movements of younger surface sediments. Wide range of cryoturbation evidences were reported in Korea [3]. Thus, we infer that the Ayajin terrace was abandoned at MIS 5a when the sea level was near the present sea level.

In the Anin area (Figs. **3**, **7**), OSL dating of sample ANIN 101, collected at 23.08 m a.s.l., yielded a depositional age of 117 ± 6 kyr and sample ANIN 102 collected at 23.09 m a.s.l. yielded a depositional age of 129 ± 8 kyr. Given that the OSL dating yields an age of ~120 kyr, the coastal terrace at Anin was likely to be established during MIS 5e. Overall, the four OSL dates provide ages for two terraces from different areas (Table **2**). These terrace ages are consistent with the morphostratigraphy of coastal terraces within the study area, and can be used to calculate regional uplift rates.

5. DISCUSSION

5.1. Spatial Distribution of Uplift Rates Deduced from Coastal Terraces

Using the ages of coastal terraces constrained by cosmogenic [10]Be and OSL dating, an uplift rate for the each study area was calculated using the height of the terrace surface, as follows:

$$U = \frac{H - SL}{A} \qquad (1)$$

where A is the age of terrace formation, SL is the global average sea level at the time of terrace formation, U is the uplift rate, and H is the average height of the paleo shoreline in coastal terraces which are reconstructed from the remnant platform surface. As elevations of original global paleo sea level highstands are not spatially uniform around the world

Table 1. Results of cosmogenic [10]Be exposure age of the Jeongdongjin coastal terrace.

Sample	Latitude (°N)	Longitude (°E)	Elevation (m Above Sea Level)	Thickness[a] (cm)	Production Rate (Atoms g[-1] yr^{-1})		Shielding[d] Factor	Denudation Rate (mm yr^{-1})	Quartz[e] (g)	Be Carrier[f] (g)	[10]Be/[9]Be (x 10^{-13})[g, h]	[10]Be Concentration (10[5] Atoms g[-1]SiO$_2$)[i,]	Age (kyr)[j, k]
					Spallation[b]	Muons[c]							
JDJ103	37.666	129.053	65.573	2	4.19	0.18	0.99	0	12.679	0.3953	3.85±1.29	8.76±0.29	211±20
JDJ104	37.666	129.053	65.573	2.5	4.17	0.18	0.99	0	19.376	0.4777	3.71±4.09	6.69±0.73	159±23
JDJ201	37.667	129.054	60.755	2	4.17	0.18	0.99	0	21.611	0.3229	8.48±8.16	9.25±0.89	224±30
JDJ202	37.667	129.054	60.755	2	4.17	0.18	0.99	0	19.219	0.4155	6.57±3.57	10.38±0.56	253±27

Note: [a]The tops of all samples were exposed at the surface.
[b]Constant (time-invariant) local production rate based on [27, 28]. A value for sea level at high latitudes (4.8 atoms [10]Be g[−1] quartz) was used.
[c]Constant (time-invariant) local production rate based on [56, 57]
[d]Geometric shielding correction for topography was measured on an interval of 10° .
[e]Density of 2.7 g cm^{−3} was used based on the granitic composition of the surface samples.
[f]Low ratio (<3x10^{-15}) Be carrier concentration of 1093.34 ppm.
[g]Isotope measurements were calibrated using KN Standard Be 0152 with a [9]Be/[10]Be ratio of 8.558 × 10^{−12} (cf. [23]) and using a [10]Be half-life of 1.387 × 10^{6} years [24, 25].
[h]Uncertainties are reported at the 1σ confidence level.
[i]Propagated uncertainties include error in the blank, carrier mass (1%), and counting statistics.
[j]Beryllium-10 model ages were calculated with the Cosmic-Ray Produced Nuclide Systematics (CRONUS) Earth online calculator [58] version 2.2 (http://hess.ess.washington.edu/).
[k]Propagated error in the model ages include a 6% uncertainty in the production rate of [10]Be and a 4% uncertainty in the [10]Be decay constant.

Table 2. Equivalent doses (De), dose rate and OSL ages of the samples

Sample	Water Content[a] (%)	Dose Rate (Gy/kyr)	Equivalent Dose (Gy)	Aliquots Used[b] (n/N)	OSL Age (kyr, 1σ SE)
AYJ-T-1	24.3 (29.0)	5.42 ± 0.13 (5.19 ± 0.12)	358±16	13/16	66±3 (69±4)
AYJ-T-2	32.1 (35.3)	4.73 ± 0.12 (4.61 ± 0.12)	330±14	16/16	70±4 (72±4)
ANIN-101	24.1 (54.0)	2.51 ± 0.13 (2.40 ± 0.12)	294±13	16/16	117±6 (147±8)
ANIN-102	24.5 (30.9)	2.50 ± 0.12 (2.41 ± 0.12)	323±17	16/16	129±8 (137±8)

Note: [a] Numbers in parenthesis were those calculated based on saturated water contents
[b] n/N refers to the ratio of (the number of aliquots used for data analysis)/(total number of aliquots loaded in the OSL measurement system).

[35-37], we used more widely accepted values: the elevation during MIS 5a was similar to the present (0 m a.s.l.), MIS 5e was a little higher (6 m a.s.l.; [30]), and MIS 7 was locally as low as 18 m a.s.l. [33].

In the JDJ area, the JDJ terrace is presently ~65 m a.s.l. and its formation age is MIS 7, thereby yielding an uplift rate of 353 mm/ky over the past ~230 kyr. Based on the OSL depositional ages of other areas, if the Ayajin terrace (tread is 19 m a.s.l) formed during MIS 5a then the uplift rate is 238 mm/ky, and if the Anin terrace (tread is 25 m a.s.l.) formed during MIS 5e then the uplift rate is 160 mm/ky over the corresponding period (Fig. **8**).

Our uplift rate is similar to the values (200-300 mm/yr) of other studies to which OSL dating was applied along the east coast of Korea [31] (Fig. **8** and Table **3**) and is the same order as short-term uplift rate (0.1-0.5 mm/yr) induced from geodetic GPS data [38].

Generally, a shore platform emerges by vertical movements, often caused by the subduction or collision of regional plates. Additionally, shore platforms can be formed by displacement along a major fault [17, 39-41]. In the southeastern area of Korea, movement along the Ulsan and Yangsan faults has affected the elevation of coastal terraces. Most of the Quaternary movement along the Ulsan and
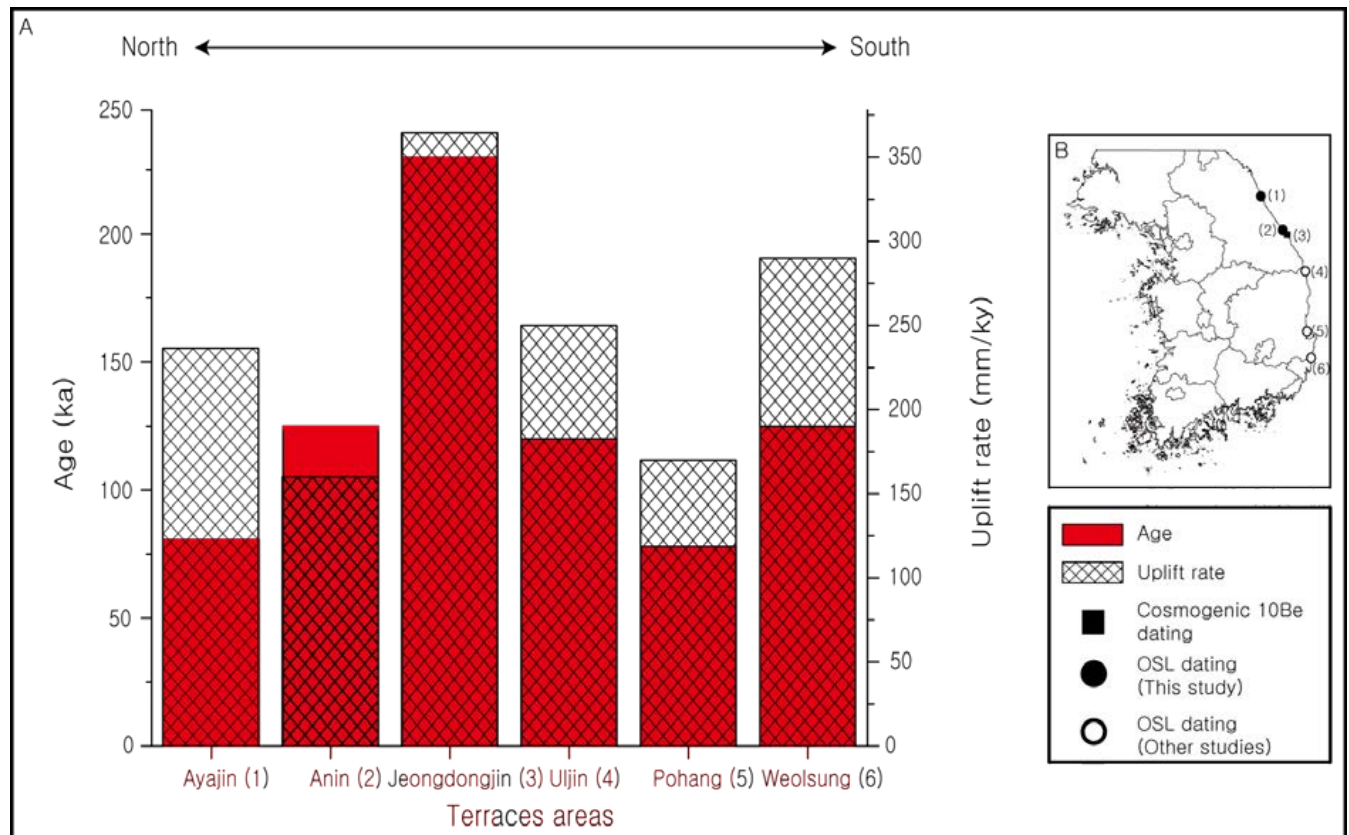

Fig. (8). (**A**) Rates of uplift deduced from coastal terraces at the study area (Jeongdongjin, Ayajin, and Anin) and other regions previously constrained by OSL dating. Along the east coast of Korea, the uplift rates induced from terraces of MIS 5a and MIS 5e look similar. Temporally, however, the uplift rate rapidly increased at ~230 kyr and subsequently decreased to the present. The uplift rate (~570 mm/kyr) at Jeongdongjin and at adjacent Anin over ~100 kyr (from MIS 7 to MIS 5e) is more than half an order of magnitude greater than the long (geologic)- and short-term denudation rate of ~80 mm/kyr in the same region [50, 51], implying that tectonic activity suddenly increased at ~230 kyr (or earlier) and that this increase lasted until ~125 kyr. (**B**) Map showing the locations for the present study and other previous studies.

Table 3.   **List of coastal terrace distributed in eastern part of Korean Peninsula, with elevation, summary of the uplift rate, and age determination methods from previous works.**

Geologic Time	Stratigraphy of Coastal Terraces Along the Eastern Coast of Korean Peninsula											
	[2]		**[15]**		**[19]**		**[16]**		**[17]**		**[18]**	
MIS 1			1st M.T.	0.5 (m)	Alluvial Plain (AP)	4–5 (m)						
MIS 3									T1 (32 kyr)	5-10 (m)		
MIS 5a	Lower M.T II; (80 kyr)	10 (m)	2nd M.T. (80 kyr)	10 (m)	Low T.3 (LT3) (73–80 kyr)	8–12 (m)	The 2nd T (73-78 kyr)	10-25 (m)	T2 (69 kyr)	15-25 (m)	T2 (60-64 kyr)	10-25 (m)
MIS 5c			3rd (T3b) (100 kyr)	20 (m)	Low T.2 (LT2) 100 kyr	14–18 (m)						
MIS 5e	Lower M.T. I (125 kyr)	18 (m)	3rd (T3a) (125 kyr)	30 (m)	Low T.1 (LT1) (125 kyr)	22–25 (m)	The 3rd T (104-127 kyr)	35-45 (m)	T3 (111-119 kyr)	30-40 (m)	T3 (116-126 kyr)	30-45 (m)
MIS 7			4th T (200 kyr)	40 (m)	Middle T.3 (MT3) (250 kyr)	32–55 (m)						
Dating method	Amino acid		OSL & C-14		OSL & Tephrochronology		OSL & C-14		OSL & C-14		OSL	
Uplift rate (mm/kyr)	100		200–300		140–220		160-320		230-310		170-300	

Yangsan faults caused by the reactivation of the Tertiary fault has been dextral strike-slip and reverse movement, which indicates spatio-temporal variations in the stress field [13, 42-46]. In the JDJ and Anin areas, no Quaternary fault displacement has been reported. However, there are a couple of examples of Quaternary fault reactivation in neighboring regions such as along the Osip-cheon Fault, located ~30 km south of the JDJ [47, 48]. Furthermore, the Kangneung Fault, located off the coast and which developed during the same period (middle Miocene) as the Yangsan and Hupo faults in southeast Korea, is likely to have been reactivated, much like its counterparts, to accommodate NNE–SSW compression during the late Quaternary [45, 46].

It is noteworthy that a substantial difference in uplift rate over the past ~125 kyr is found on the west and east coasts across central Korea. Extensive, successive shore platforms exist along the west coast of the Korea Peninsula to the present sea level. In the Anmyeon Island area (Fig. **1**), [10]Be surface exposure ages of the shore platform demonstrate that it is as old as MIS 5e (or even older), implying that the shore platform found near the present sea level was established in the last interglacial period (MIS 5). Given the age and the elevation of the shore platform surface, it has been noted that the western coast of central Korea has experienced little uplift over the last ~125 kyr [49]. It is likely that the west and east coasts of central Korea have been differentially uplifted under different tectonic regimes [45, 46].

5.2. Temporal Variations in Uplift Rate

Our uplift rates are similar to the incision rate in the Osip-cheon area (Fig. **1**), located <30 km to the southwest of the study area. In the Osip-cheon area, the uplift rate has decreased over the past 200 kyr, and ranges from approximately 280 to 170 mm/kyr with an average rate of ~240 mm/kyr [48]. Similar uplift rates deduced from fluvial and coastal terraces between the study area and the adjacent,

Osip-cheon area imply that the central-east coastal area of Korea experienced similar tectonic forces that declined in magnitude towards the present over the past 200 kyr.

The calculated uplift rate (~350 mm/ky) of JDJ over the past 230 kyr is 3–5 times higher than the long-term exhumation rate based on single-grain (U–Th)/He thermochronology data for the Daegwanryeong area, located <20 km west of the present study area ([50]; Fig. **1**). They suggested that rapid exhumation at ca. 22–20 Ma related to the opening of the East Sea (or Japan Sea) and that the cooling rate corresponds to an exhumation rate of ~80 mm/kyr. This is an average exhumation rate over the past ~22 Ma, and the rate may have been variable during shorter intervals. Interestingly, the short-term (10^5–10^6 years) denudation rate of eastern Korea constrained by the abundances of cosmogenic [10]Be on riverine sediments is very similar to the long-term rates of denudation (or exhumation) [51], suggesting that eastern Korea is moving towards a new geomorphic equilibrium forced by Quaternary tectonic uplift. Given that the study areas located along the central-east coast of Korea have experienced similar tectonic forces (particularly the JDJ and Anin areas, which are only ~5 km apart), the regional uplift rate is assumed to be ~592 mm/kyr over the past ~100 kyr (MIS 7 to MIS 5e), which is ~5 times higher than the long-term (~20 Ma) and short-term (~30 kyr) rates of ~80 mm/kyr. This change in uplift rate reflects the fact that the tectonic force in central-east Korea showed a rapid increase between ca. 220 and 123 kyr before slowing to the present day. The causes of the rapid uplift over at least the past 200 kyr may be due to variations in the dominant stress regime. The Korean Peninsula has undergone multiple tectonic deformation throughout the Cenozoic, mainly from E-W extension to E-W compression [45]. During the Quaternary, the Korean Peninsula was generally under the influence of an E–W or ENE–WSW compressional stress regime due to the decrease in

subduction angle of the Pacific plate and eastward movement of the Amurian plate [52].

CONCLUSION

The JDJ coastal terrace has been a focus of coastal terrace research over the past half century. Despite many efforts to establish the absolute timing of the terrace stratigraphy along the central-east coast of Korea, there has yet to be an unequivocal consensus, due to an absence of absolute dating of the old (>MIS 5e) surface. Thus, we firstly applied [10]Be cosmogenic surface exposure dating to constrain the age of the old JDJ terrace surface as well as conventional OSL dating to the low, young coastal terraces at Ayajin and Anin. Our age data suggest that the JDJ terrace surface was established during MIS 7 and that the Ayajin and Anin terraces formed during MIS 5a and MIS 5e, respectively. Using a paleo sea level of −18 m, 0 m a.s.l., and 6 m a.s.l. for the MIS 7, MIS 5a, and MIS 5e sea level highstands, respectively, we infer uplift rates of 353, 258, and 159 mm/kyr for each area over the corresponding time periods. The temporal trend in uplift rates derived from the coastal terraces is similar to the trend inferred from fluvial terraces in adjacent areas, suggesting that our results are reasonable and that the region has experienced a similar recent tectonic history. The uplift rate of the central-east part of Korea (200–300 mm/kyr) is similar to that of the southeastern part of Korea, but is substantially great relative to the western part of central Korea, which has experienced little uplift over this time period. It is likely that the study area has been affected by a similar tectonic regime as southeastern Korea, but has been affected by a significantly different tectonic setting from the western part of central Korea. The temporal rates of uplift obtained in the present study demonstrate that the rate of uplift over the past 230 kyr is 3–5 times faster than the long- and short-term denudation rates (~80 mm/kyr for ca. 22 Myr and ca. 30 kyr). Uplift rates reached a maximum (~600 mm/kyr) no later than ~MIS 7. Increase in the rate of uplift in study area were possibly related to a change in the regional tectonic inversion from NW–SE transtension to NNE–SSW transpression which initiated in late Tertiary to early Quaternary.

CONFLICT OF INTEREST

The authors confirm that this article content has no conflict of interest.

ACKNOWLEDGEMENTS

REFERENCES

[1]   Hwang MI. Topographic study of flat surfaces along the coast of Cheong Dong area, east coast of Korea. Master thesis, Seoul National University, Seoul, Korea 1966.

[2]   Hong SC, Choi JH, Yeo EY, Kim JW. Principles of K-Feldspar IRSL (InfraRed Stimulated Luminescence) Dating and Its Applications. J Geol Soc Korea 2013; 49: 305-24.

[3]   Choi SG. Tectonic Movement indicated by the Pleistocene Palaeoshoreline in the Eastern Coast of Korea. Trans Jpn Geomorphol Union 2001; 22: 265-75.

[4]   Yi SB, Tustomu S, Fusao A. New discovery of Aira-Tn Ash (AT) in Korea. J Korean Geograph Soc 1998; 33: 447-54.

[5]   Yi SB, Lee YI, Lim HS. Characteristics and depositional environment of paleosol layers developed on top of the terrace in the Jeongdongjin area, East Coast, Korea. Korean J Quat Res 2009; 23: 1-24.

[6]   Auclair M, Lamothe M, Huot S. Measurement of anomalous fading for feldspar IRSL using SAR. Radiat Measure 2003; 37: 487-92.

[7]   Lian OB, Roberts RG. Dating the Quaternary: Progress in luminescence dating of sediments. Quat Sci Rev 2006; 25: 2449-68.

[8]   Stone J, Lambeck K, Fifield LK, Evans JM, Cresswell RG. A lateglacial age for the main rock platform. West Scotland Geol 1996; 24: 707-10.

[9]   Alvarez-Marrón J, Hetzel R, Niedermann S, Menendez R, Marquinez J. Origin, structure and exposure history of a wave-cut platform more than 1 Ma in age at the coast of northern Spain: A multiple cosmogenic nuclide approach. Geomorphology 2008; 93: 316-34.

[10]   Korea Meterological Administration. Climatic data of Korea over 30 years 2010.

[11]   Jin S, Park P-H. Strain accumulation in South Korea inferred from GPS measurements. Earth Planets Space 2006; 58: 529-34.

[12]   Na HW, Chang CD, Chang CJ. Friction-dependent slip behavior of Imgok fault under the present-day stress field. J Eng Geol 2013; 23: 217-25.

[13]   Park JC, Kim W, Chung TW, *et al*. Focal mechanisms of recent earthquakes in the Southern Korean Peninsula. Geophys J Int 2007; 169: 1103-14.

[14]   Kyung JB, Huh SY, Do JY, Cho DR. Relation of intensity, fault plane solutions and fault of the January 20, 2007 Odaesan Earthquake (ML = 4.8). J Korean Earth Sci Soc 2007; 28: 202-13.

[15]   Ko MS, Chang CD, Lee JB, Shim TM. Application of Coulomb Stress Model to the Odaesan earthquake and its aftershock distribution. J Geol Soc Korea 2009; 45: 741-50.

[16]   Jung MS, Kim KY, Huh S, Kim HJ. Identification of Quaternary fault and shallow gas pockets through high-resolution reprocessing in the East Sea, Korea. J Korean Geophys Soc 1999; 2: 39-44.

[17]   Choi SJ, Merritts DJ, Ota Y. Elevations and ages of marine terraces and late Quaternary rock uplift in southeastern Korea. J Geophys Res 2008; 113: B10403.

[18]   Kim JW, Chang HW, Choi JH, Choi KH, Byun JM. The morphological characteristics and geochronological ages of coastal terraces of Heunghae region in northern Pohang City, Korea. J Korean Geomorphol Assoc 2005; 12: 103-16.

[19]   Kim JW, Chang HW, Choi JH, Choi KH, Byun, JM. Optically Stimulated Luminescence dating on the marine terrace deposits of Hujeong-Jukbyeon region in Uljin, Korea. J Korean Geomorphol Assoc 2007; 14: 15-27.

[20]   Kim JW, Chang HW, Choi JH, Choi KH, Byun JM. Landform characteristics of coastal terraces and optically stimulated luminescence dating on the terrace deposits in Yangnam and Yangbuk area of the Gyeongju city, South Korea. J Korean Geomorphol Assoc 2007; 14: 1-14.

[21]   Kim JY, Oh KC, Yang DY, *et al*. Stratigraphy, chronology and implied uplift rate of coastal terrace in the southeastern part of Korea. Quat Int 2008; 183: 76-82.

[22]   Kohl CP, Nishiizumi K. Chemical isolation of quartz for measurement of in-situ produced cosmogenic nuclides. Geochim Cosmoch Acta 1992; 56: 3583-7.

[23] Nishiizumi K, Imamura M., Caffee M, *et al*. Absolute calibration of [10]Be AMS standards. Nuclear Instruments and Methods in Physics Research–Beam Interactions with Materials and Atoms 2007; 258B: 403-13.

[24] Chmeleff J, von Blanckenburg F, Kossert K, Jakob D. Determination of the [10]Be half-life by multicollector ICP-MS and liquid scintillation counting. Nuclear Instruments and Methods in Physics Research Section B: Beam Interactions with Materials and Atoms 2010; 268: 192-9.

[25] Korschinek G, Bergmaier A, Faestermann T, *et al*. A new value for the half-life of [10]Be by Heavy-Ion Elastic Recoil Detection and liquid scintillation counting. Nuclear Instruments and Methods in Physics Research Section B: Beam Interactions with Materials and Atoms 2010; 268: 187-91.

[26] Balco G, Stone JO, Lifton NA, *et al*. A complete and easily accessible means of calculating surface exposure ages or erosion rates from [10]Be and [26]Al measurements. Quaternary Geochronol 2008; 3: 174-95.

[27] Lal D. Cosmic ray labeling of erosion surfaces: In situ nuclide production rates and erosion models. Earth Planet Sci Lett 1991; 104: 429-39.

[28] Stone JO. Air pressure and cosmogenic isotope production. J Geophys Res 2000; 105: 753-9.

[29] Murray AS, Wintle AG. Luminescence dating of quartz using an improved single-aliquot regenerative-dose protocol. Radiat Measure 2000; 32: 57-73.

[30] Murray AS, Olley JM. Precision and accuracy in the optically stimulated luminescence dating of sedimentary quartz: a status review. Geochronometria 2002; 21: 1-16.

[31] Choi JH, Murray AS, Cheong CS, Chang HW. Luminescence dating of well-sorted marine terrace sediments on the southeastern coast of Korea. Quat Sci Rev 2003; 22: 407-21.

[32] Chappell J, Shackleton NJ. Oxygen isotopes and sea level. Nature 1986; 324: 137-40.

[33] Shackleton NJ. 1987. Oxygen isotopes, Ice volume and sea level. Quat Sci Rev 1987; 6: 183-90.

[34] Kanamori H, Brodsky EE. The physics of earthquakes. Phys Today 2001; 54: 34-40.

[35] Dutton A, Bard E, Antonioli F, Esat TM, Lambeck K, McCulloch MT. Phasing and amplitude of sea-level and climate change during the penultimate interglacial. Nature Geosci 2009; 6: 355-9.

[36] Muhs DR, Simmons KR, Schumann RR, Halley RB. Sea-level history of the past two interglacial periods: new evidence from U-series dating of reef corals from south Florida. Quat Sci Rev 2011; 30: 570-90.

[37] Rohling EJ, Grant, K, Bolshaw, M, *et al*. Antarctic temperature and global sea level closely coupled over the past five glacial cycles., Nature Geosci 2009; 2: 500-4.

[38] Hamdy A, Park P-H, Jo B. Vertical velocity from the Korean GPS Network (2000-2003) and its role in the South Korean neo-tectonics. Earth Planets Space 2007; 59: 337-41.

[39] Ota Y, Omura A. Contrasting styles and rates of tectonic uplift of coral reef terraces in the Ryukyu and Daito islands, southwestern Japan. Quat Int 1992; 15-16: 17-29.

[40] Zazo C, Silva PG, Goy JL, *et al*. Coastal uplift in continental collision plate boundaries: Data from the Last Interglacial marine terraces of the Gibraltar Strait area (south Spain). Tectonophysics 1999; 301: 95-109.

[41] Marquardt C, Lavenu A, Ortlieb L, Godoy E, Comte D. Coastal neotectonics in southern central Andes: Uplift and deformation of marine terraces in northern Chile (27S). Tectonophysics 2004; 394: 193- 219.

[42] Kyung JB, Lee K, Okada A, *et al*. Study of fault characteristics by trench survey in the Sangcheon-ri area in the southerarn part of Yangsan Fault, southeastern Korea. J Korean Earth Sci Soc 1999; 20: 101-10.

[43] Chang TW. Quaternary tectonic activity at the eastern block of the Ulsan fault. J Geol Soc Korea 2001; 37: 431- 44.

[44] Kyung JB, Chang TW. The latest fault movement on the northern Yangsan fault zone around the Yugye-ri area, southeast Korea. J Geol Soc Korea 2001; 37: 563-77.

[45] Ree JH, Lee YJ, Rhodes EJ, *et al*. Quaternary Reactivation of Tertiary faults in the southeastern Korean Peninsula: Age constraint by optically stimulated luminescence dating. Island Arc 2003; 12: 1-12.

[46] Park Y, Ree JH, Yoo SH. Fault slip analysis of Quaternary faults in southeastern Korea. Gondwana Res 2006; 9: 118- 25.

[47] Ree JH. Report on the active fault along the Youngdong railroad. Unpublished report 1998: 1-32.

[48] Lee SY, Seong YB, Shin YK, *et al*. Cosmogenic [10]Be and OSL dating of fluvial strath terraces along the Osip-cheon River, Korea: tectonic implications. Geosci J 2011; 15: 349-444.

[49] Choi KH, Seong YB, Jung PM, Lee SY. Using Cosmogenic [10]Be dating to unravel the antiquity of a rocky shore platform on the West Coast of Korea. J Coast Res 2011; 28: 641-57.

[50] Min K, Cho M, Reiners PW. Coeval exhumation of Korean Peninsula and opening of East Sea revealed from single-grain (U-Th)/He thermochronology. Thermo 2010 Abstracts: 265.

[51] Kim DE, Seong YB, Byun JM. Transient landscape in quiescent land: a case study from Korea. Global Planetary Change 2015: Under review.

[52] Son M, Kim JS, Jung HY, Lee YH, Kim IS. Characteristics of the Cenozoic crustal deformation in SE Korea and their tectonic implications. Korean J Petrol Geol 2007; 13: 1-16.

[53] Korea Institute of Geoscience and Mineral Resources. Geological Map of Gangeung and Sanseongu 1962.

[54] http://www.ujeil.com/news/articleView.html?idxno=38691. [Accessed on October 31, 2014].

[55] Evans JW. Growth Rate of the Rock-Boring Clam Penitella Penita (Conrad 1837) in relation to hardness of rock and other factors. Ecology 1968; 49: 619-28.

[56] Heisinger B, Lal D, Jull T, *et al*. Production of selected cosmogenic radionuclides by muons: 1. fast muons. Earth Planet Sci Lett 2002; 200: 345-55.

[57] Heisinger B, Lal D, Jull T, *et al*. Production of selected cosmogenic radionuclides by muons: 2. Capture of negative muons. Earth Planet Sci Lett 2002; 200: 357-69.

[58] Balco G. 2009. CRONUS [10]Be-[26]Al Exposure Age Calculator Version 2.2. [Cited 2014 March 15]. Available from: http://hess.ess.washington.edu/math/